WATER RESOURCES RESEARCH, VOL. 35, NO. 2, PAGES 427–434, FEBRUARY 1999

Lateral expansion of preferential flow paths in sands

David A. DiCarlo

Department of Petroleum Engineering, Stanford University, Stanford, California

Tim W. J. Bauters, Christophe J. G. Darnault, Tammo S. Steenhuis, and J.-Yves Parlange

Department of Agricultural and Biological Engineering, Cornell University, Ithaca, New York

Abstract. The stability and persistence of preferential flow paths in sands can determine the flow paths of subsequent infiltration events. We have measured the evolution of preferential flow paths in a slab of sandy soil using an array of tensiometers and light transmission. The pressure and water content measurements show that the nonuniform moisture content exists even when the potentials are equalized horizontally and that then are the result of hysteresis in the soil's pressure-saturation relationship. The equalization of potential takes place over several days, if at all, and is consistent, initially, with estimates of vapor transport out of the finger cores. Once the soil is wet enough, the remainder of water movement takes place in liquid films. Hysteresis produces another interesting situation when the pack is drained. We find that the wetter portions of the soil can be at a lower potential than the drier portions, resulting in a horizontal driving force for a flow of water from the drier to the wetter soil.

1. Introduction

Subsurface preferential flow of water, in which small areas of the subsurface carry large portions of the flow, has been observed in a variety of soils [*Hill and Parlange*, 1972; *Beven and Germann*, 1982; *Glass et al*., 1987, 1989; *Baker and Hillel*, 1990; *Ritsema and Dekker*, 1994]. As preferential flow provides a mechanism to bypass most of the porous media, the effects include enhanced solute transport, less filtering and adsorbing of contaminants in the soil, and fast travel to groundwater or tile lines. Preferential flow can result from macropores and other inhomogeneities [*Beven and Germann*, 1982], but it has also been observed in uniform soils with uniform rainfall and low application rates [*Selker et al*., 1992a]. In this case, preferential flow is created from the lack of stability of the invading water front [*Raats*, 1973; *Parlange and Hill*, 1976].

Preferential flow also creates a nonuniform moisture profile in the soil. The soil within the initial preferential flow paths (similarly called fingers) will remain wetter than the soil outside of the fingers. The persistence or horizontal spreading of this nonuniform water content will affect subsequent infiltration events. *Glass et al*. [1989] found that in laboratory sandy soils, nonuniform water contents remained after 2 weeks of continuous infiltration. Subsequent infiltrations followed the old finger paths, resulting in persistent preferential flow. Conversely, if the soil is uniformly wet, *Liu et al*. [1994] found that the finger widths are much greater, and *Diment and Watson* [1985] and *Lu et al*. [1994] found that preferential flow might even be completely inhibited. In field soils, *Ritsema and Dekker* [1994] found that over a calendar year the finger paths could vary greatly in diameter, sometimes involving more of the soil and lessening the effects of preferential flow. Clearly, the evolution of the initial nonuniform moisture profile plays a large role in the wetting front stability of subsequent infiltrations.

When the nonuniform moisture profile is produced, it is natural to assume that water will diffuse out of the fingers into the drier soil. *Glass et al*. [1989] hypothesized that this does not occur at an appreciable rate because hysteresis in the pressure-saturation relationship can yield different moisture contents at the same water potential. This occurs if the portion of the soil inside the initial finger path (from here on called the finger core) is on the drying branch of the pressure-saturation relationship, while the soil outside the finger core is on the wetting branch. *Philip* [1991] and *Raats and van Duijn* [1995] later hypothesized that hysteresis can cause the effective water diffusivity to become zero or even negative for a range of water contents. In any case, the horizontal redistribution of water after a preferential flow event can provide a unique system for studying water flow where hysteresis in the pressure-saturation relation plays a large role.

In this paper we describe measurements of the water potential and water saturation within a soil during the redistribution of water after a nonuniform water profile is produced from fingered flow. Potentials were measured along two rows using an array of miniature tensiometers, and water saturations were measured using light transmission through the soil slab. The redistribution rate of water is consistent with rough estimates of vapor transport of the water. We definitively show that the hysteresis in the soil's pressure-saturation relationship is the reason why a nonuniform moisture profile exists even when the water potential is uniform. Also, hysteresis is found to create a unique situation where the wetter portions of the soil are at a lower potential than adjacent drier portions.

2. Materials and Methods

Experiments were carried out in a sand-packed two-dimensional chamber of height 55 cm, width 30 cm, and interior thickness 1.2 cm. Sixteen tensiometer ports and four small

Paper number 1998WR900061.
0043-1397/99/1998WR900061$09.00

screen-covered holes were drilled into the chamber's front face. The holes produced an air connection to the atmosphere so the air had an exit path during the infiltrations. The chamber was packed using a dual-sieve randomizer with cleaned, sieved quartz sand (Unimin Corporation). The sieved sand was labeled 20/30 because it passed through a size 20 sieve (20 wires per inch) but not through a size 30 sieve, and thus it had sand diameters between 0.60 and 0.84 mm.

Water contents were obtained using a light transmission technique, in which a bank of fluorescent lights is used to illuminate the sand-packed chamber from behind [*Glass et al*., 1989]. As the index of refraction for water compares to the index of refraction for sand, the light transmitted through the sand pack increases monotonically with the water saturation. The transmitted light was recorded with a video camera and images were computer analyzed for light intensity via a frame grabber board. The relationship between transmitted light intensity and water content was measured prior to the infiltration experiments through the following procedure, suggested by *Bell et al*. [1990]. The experimental chamber was saturated from below with water and allowed to drain. Several video images of this drained profile were taken and a relationship between the transmitted intensity and vertical position was measured. Subsequently, the front of the chamber was removed, and water content versus height was measured by removing sand at each vertical position and oven drying it. The curves were merged to provide the water content versus light intensity calibration curve. For both sands the transmitted light increased linearly with the water content up to water contents of 0.30 cm^3/cm^3. Above 0.30 cm^3/cm^3 the transmitted light increased much more slowly with water content. From the scatter in the data we estimate that the standard deviation in the water content is roughly 0.01 cm^3/cm^3 for water contents below 0.30 cm^3/cm^3 and 0.03 cm^3/cm^3 for water contents above 0.30 cm^3/cm^3.

Water pressures were obtained at 16 separate positions within the chamber using 16 miniature tensiometers. Figure 1 shows a schematic representation of the chamber and the tensiometer positions. As we were interested in lateral movement of the fingers, the tensiometers were threaded into the chamber along two horizontal lines of eight tensiometers each, with the tensiometer centers separated by 2 cm. Each tensiometer consisted of a hollow brass housing filled with water. One end was connected to the soil through a sealed 0.8 cm stainless steel porous plate (sintered particle size of 2 μm), and the other end was connected to a pressure transducer through a rigid plastic tube and a three-way valve. The other port of each three-way valve was connected to a vertical reservoir of water. Prior to each experiment, the valve was opened to the reservoir, and the transducers were calibrated using different water heights in the reservoir. After calibration the water pressure inside the tensiometers was set to -5 cm of water, to minimize leakage of water from the tensiometers into the dry sand. The tensiometer readings were stable to approximately 0.2 cm of water, but we estimate a standard deviation of 1 cm of water owing to the finite size of the porous plate.

Before the infiltrations began the bottom 5 cm of the chamber was filled with water from below and subsequently allowed to drain. This was done for two reasons. First, when the infiltration reached the bottom water layer, the water could drain without changing the bottom water profile and thus kept the bottom boundary condition constant. Second, this produced a region of saturated sand to calibrate out any possible temporal variations in the light intensity. For the infiltrations, water was applied uniformly at the soil surface at a rate of 9 cm/hr. The application system consisted of a peristaltic pump–driven point source attached to a rotating camshaft that moved the source continuously across the soil surface. To eliminate the possible flow down the side edges of the chamber, gutters were installed to prevent rain from impacting within 2 cm of the chamber edges. As a result, the only observed flow paths were through the uniformly packed sand. The application of water was continued for 10 days, or until the water pressures equalized. When the application was ceased, the chamber was drained for 24 hours, after which the application was restarted.

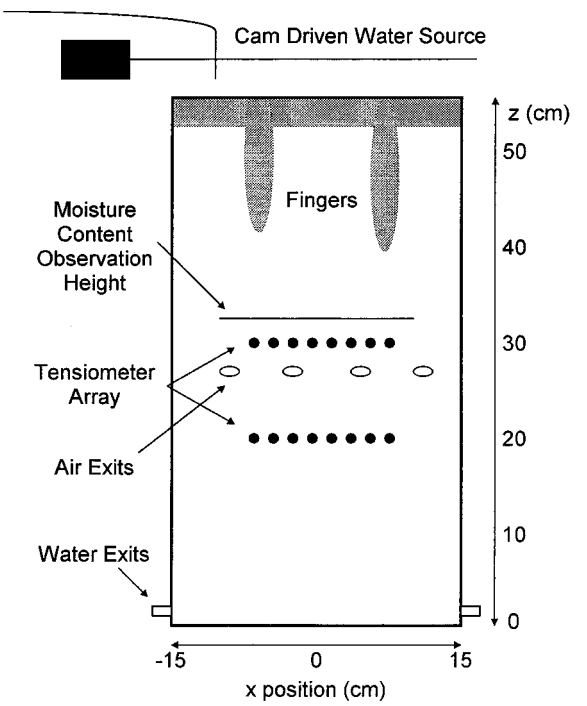

Figure 1. A schematic of the experimental chamber. Water contents were measured along several elevations; the results shown are water contents from the line. Pressure readings were made by the two rows of eight tensiometers each.

At the start of each infiltration the low-intensity uniform rain at the soil surface quickly produced fingered flow and a nonuniform water profile within 2 cm of the surface. Initially, only one or two fingers were produced, but within 2 hours four or five fingers were observed within the chamber. From that point onward this finger pattern remained roughly constant until the water application was stopped. Video images of the chamber (and thus water contents) were measured continuously for the first 15 min when the initial finger (or fingers) traversed the chamber. During run 1, images were obtained for the first 24 hours, but this produced excess heating in the rear of the chamber, so for the rest of this run and subsequent runs the lights were turned off. Instead, images were obtained several times a day until the application was halted.

In the data analysis, images were grabbed for analysis every 15 s when the fingers were quickly traveling downward. During the slow sideways diffusion, images were grabbed for analysis a few times a day. From these images, horizontal lines of pixels 2 cm above and below each tensiometer bank were obtained, and the pixel intensity was converted into water content versus

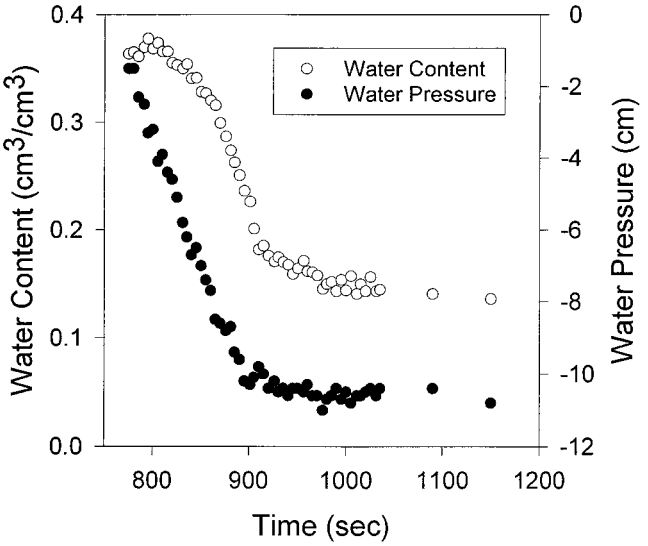

Figure 2. Water contents and pressures obtained for an initial finger during run 2 from the point where the finger enters the observation region. Pressure-saturation relationships for the drying curve can be obtained from the data, and the results are identical to those observed by *Liu et al*. [1994].

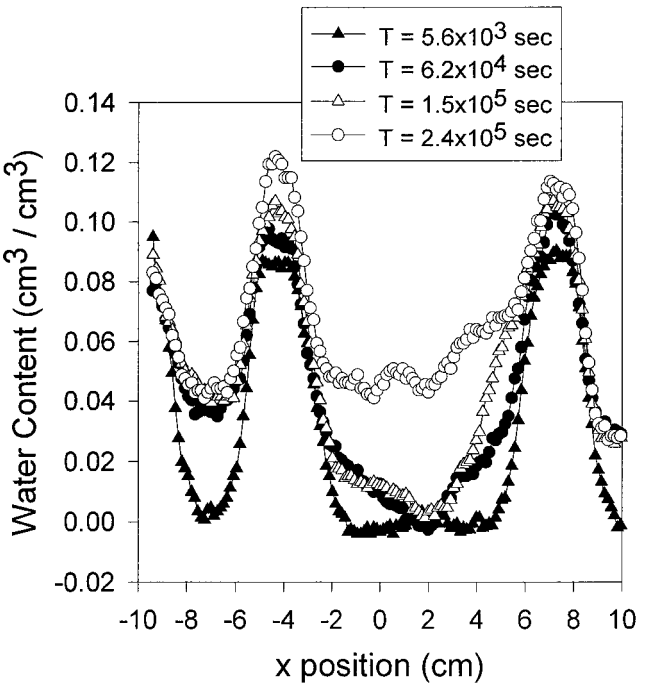

Figure 3. Water profiles at various times after passage of the fingers during run 2. The water content outside the finger cores slowly rises throughout the experiment.

horizontal position. Pressure data were collected continuously for the whole infiltration at the positions of the 16 tensiometers.

3. Results

Many experimental runs were attempted, but only three resulted in uniform packings (no inhomogeneities observed in light transmission through the dry chamber) and accurate tensiometer readings (no bubbles or leaks from any tensiometer). These three runs were performed in October 1995 (run 1), December 1995 (run 2), and January 1997 (run 3). In the experiments the initial finger had water contents, water pressures, and widths identical to those observed by *Selker et al*. [1992b] and *Liu et al*. [1994]. Figure 2 shows both the measured water content and pressure (taken 2 cm below the observed water content) versus time for an initial finger. The finger tip was at or near saturation, and behind it the water content decreased quickly. The tensiometers showed a decreasing water pressure after the tip of the finger passed. Thus, after the initial wetting, the region within the original finger path was on a drying portion of the pressure-saturation curve, and the pressure and saturation data can be combined to yield a drying curve for the soil.

Within a couple of hours, several more fingers reached the bottom of the chamber, with an average spacing of 6–10 cm and widths of 2–3 cm. After these relatively quick forming fingers reached the bottom, the water profile and pressures inside the chamber changed much more slowly. Surprisingly, the subsequent changes varied for the different experimental runs. In run 1, portions of the soil remained air dry after 10 days, and the horizontal pressures did not equilibrate. In runs 2 and 3, close to the entire soil became wetted after 4 days, and the horizontal pressures equilibrated. The details of the runs are described as follows, beginning with the later runs.

For runs 2 and 3, within 6 hours after the infiltration began, partially wet fringes could be observed around each finger core, and within 2 days the fringes had steadily grown to fill the entire chamber with at least some moisture. Figure 3 shows the horizontal moisture profile 2 cm above the upper set of tensiometers at various times during run 2. Run 3 produced similar results as those shown in Figure 3.

Concurrent with the finger expansion, the pressures outside the finger paths increased until at every tensiometer the pressures were equal across the tensiometer line. Figure 4 shows the pressure data from the upper tensiometers versus time for run 2, after the initial fingers passed. For tensiometer positions within the finger cores (solid symbols), the pressure remained a relatively constant −10 cm. For tensiometer positions outside the finger cores (open symbols), the measured pressure dropped from the (unphysical) initial set point of −10 cm to values reaching less than −100 cm. After this decrease the measured pressure slowly increased until coming to equilibrium with the measured pressure in the initial fingers. For these tensiometers we consider the measured pressure to be accurate only when the pressure is increasing. This is because when a tensiometer is connected to air dry soil, the water inside the tensiometer casing is not in contact with any water within the soil. Thus the initial measured pressure is whatever the user sets the pressure in the tensiometer casing to be and is not the actual pressure in the soil. The measured pressure drops slowly in an effort to equilibrate with the extreme negative pressure of the air dry soil. The only way for the measured pressure to start increasing is when the actual pressure in the soil begins to increase.

After the tensiometer values equalized (to within 2–3 cm), no more changes in the tensiometer values or water moisture profiles were observed for the next 24 hours. Thus we assumed that horizontal flow had stopped and that the final nonuniform moisture profile was stable. These differences in moisture content can be explained simply in terms of hysteresis in the

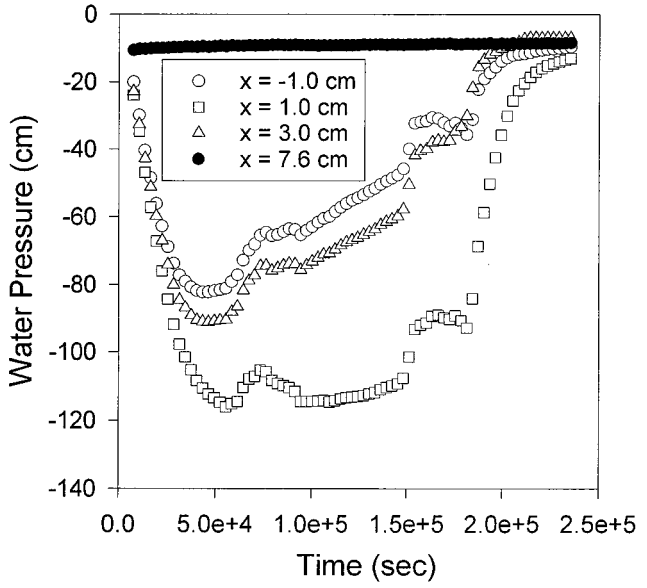

Figure 4. Water pressures versus time for four of the tensiometers after passage of the fingers during run 2. The legend depicts the x position of each of the tensiometers shown. Solid symbols are for tensiometers within the finger cores, and open symbols are for tensiometers outside the finger cores. The pressures outside the finger cores slowly equalize with time.

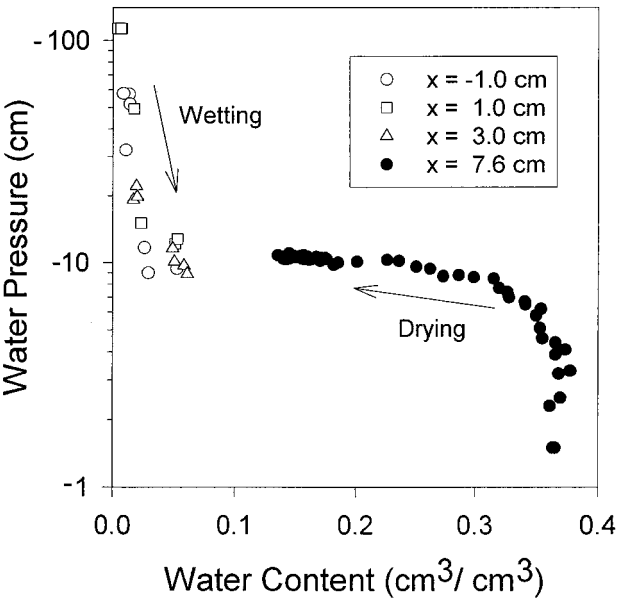

Figure 5. The pressure saturation curves obtained from combining the water contents at water pressures at various tensiometer positions for run 2. Solid symbols are for tensiometers within the finger cores, and open symbols are for tensiometers outside the finger cores. Along the same row it can be seen that tensiometers within the cores are on the drying curve and tensiometers outside the cores are on the wetting curve.

pressure-saturation curve, as the finger cores are on the drying branch of the pressure-saturation curve and thus hold much more water at equal pressure than outside the fingers, where the soil is on the wetting branch. This is detailed below.

The pressure and moisture data can be merged to produce a pressure-saturation relationship for the soil at each tensiometer position. Figure 5 shows the observed pressure-saturation relationship for data points on the top row of the tensiometers for run 2. The pressure of the points within the finger core increased, initially, rapidly at the wetting front of the tip to -1.5 cm (wetting; not shown) and then decreased from -1.5 to -10 cm at equilibrium (drying), while the points outside the initial fingers increased from, initially, over -70 cm to -10 cm at equilibrium (wetting). In this case there are very different timescales for these processes. The wetting and dying to equilibrium inside the fingers took place in less than an hour, while the wetting to equilibrium outside the fingers took place over several days. Thus the wetting and drying regions exist adjacently within the same soil. When equilibrium is reached at these pressures, there exists a moisture difference of roughly 0.07 cm^3/cm^3 between the wetting (outside) and drying (inside) curves of the finger.

In this final equilibrium state the nonuniform water content implies nonuniform conduction of the applied water. Assuming a *Brooks and Corey* [1964] relationship for the conductivity,

$$\frac{K(\theta)}{K_s} = \left(\frac{\theta}{\theta_s}\right)^{\alpha} \tag{1}$$

where $\alpha = 3.4$ for 20/30 sand [*Liu et al.*, 1994], the observed difference of water content yields an unsaturated conductivity roughly 30 times greater inside the cores than outside. Using the ratio of the cross-sectional area inside the cores to the cross-sectional area outside the cores, we estimate that over 95% of the vertical flow is still contained within the initial fingers. An apparently stable water distribution can still yield extremely preferential flow.

In runs 2 and 3, 24 hours after pressure equilibrium was reached, the infiltration was stopped. The soil subsequently dried through drainage out the bottom. Figure 6 shows how the pressure changes along the top row of tensiometers. The pres-

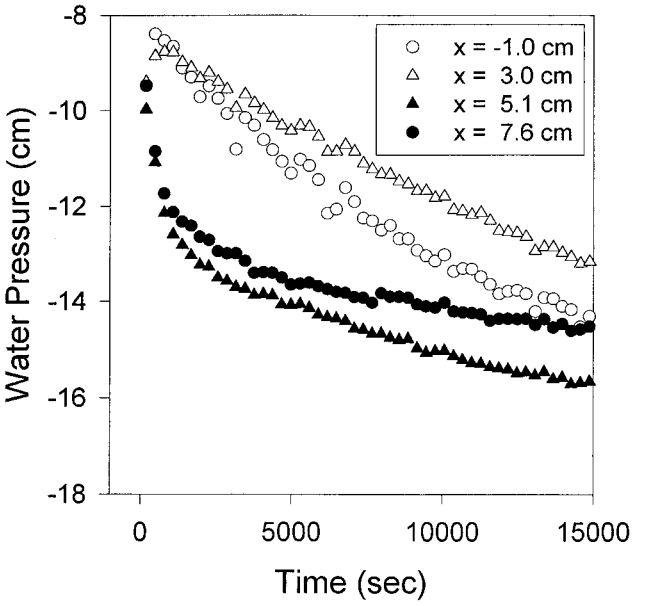

Figure 6. Pressures at four tensiometer positions after pressure equilibrium is reached and the infiltration is ceased (at time, $T = 0$). Pressures inside the cores (solid symbols) drop faster than pressures outside the cores (open symbols).

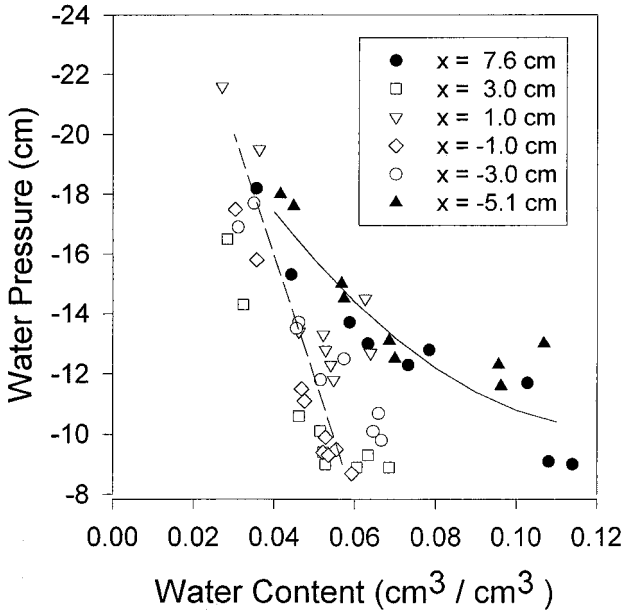

Figure 7. Pressure-saturation relationships on the draining of the chamber. Solid symbols are for tensiometers within the finger cores, and open symbols are for tensiometers outside the finger cores. The lines are guides for the eye. On drainage the different tensiometer positions all end up at the point on the pressure saturation curve.

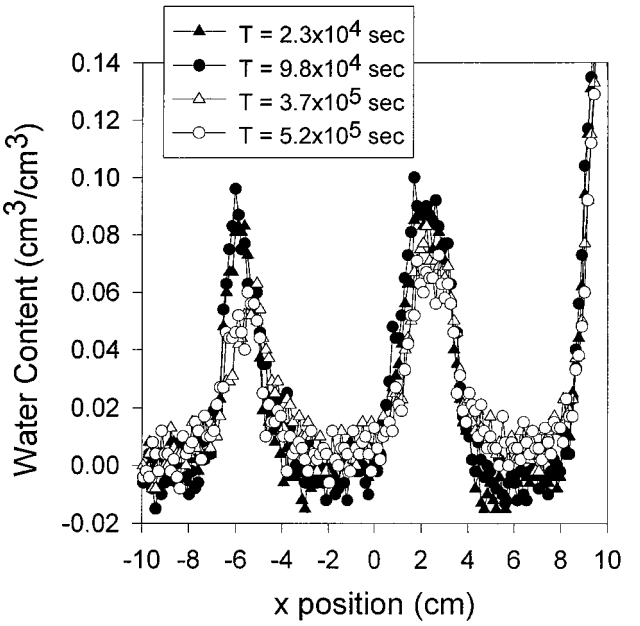

Figure 8. Water profiles at various times during run 1. The water content outside the finger cores remains very low throughout the experiment.

sure within the cores drops faster than that outside the cores owing to the higher conductivity in the cores. But the water content remains generally higher within the cores, as can be seen in Figure 7, which shows the pressure-saturation relationship at the soil positions behind the top row of tensiometers on drying. This leads to an unique situation where the pressure is higher where there is less water content, and thus there is a pressure gradient drawing water from the drier regions into the wetter regions. To clarify this, we consider the situation at 5000 s after the water application was stopped. Figure 6 shows that the pressure inside the finger is almost -14 cm (closed symbols), which is almost 4 cm lower than the pressure outside the finger (open symbols). Using these pressures in Figure 7, we note that the moisture content at a pressure of -14 cm inside the finger is almost 0.01 cm^3/cm^3 higher than the moisture content outside the finger at -11 cm pressure. Hence water moves from the higher pressure with the lower moisture content outside the finger to the higher moisture content with the lower pressure.

Twenty-four hours after the infiltration was stopped, it was restarted at the same rate. Upon reinfiltration the water content became much more uniform. The infiltrating water still tended to flow preferentially along the old finger paths, but it appeared that the finger widths were so large such that space between adjacent old finger paths was covered with the new fingers, and the wetting front completely filled the chamber. The horizontal water content was much more uniform than before, with water contents ranging from 0.07 to 0.09 cm^3/cm^3. Along each row tensiometer readings equilibrated in less than 1 hour.

For run 1, after the first 24 hours of continuous lighting, water was observed to condense on the front face of the chamber (away from the lights) where the tensiometers were located. Also, after 24 hours, the observed pressures equalized, ostensibly owing to the condensation. This was an artifact of the heating, because when the lights were turned off, the pressures outside the fingers dropped to equilibrate with the dry soil behind them. Importantly, after 10 days of infiltration, there were still large portions of air dry sand, and the finger fringes were not increasing at any observable rate. Figure 8 shows the time evolution of the horizontal moisture profile directly above the upper set of tensiometers from run 1. As for the other runs the pressure data followed that observed in the water content data. Figure 9 shows the pressure data from the upper tensiometers versus time (after the lights were turned off) for run 1. Pressures outside of the finger cores do not equilibrate with the pressure inside the cores and never begin increasing.

In this case, although the pressures did not equalize, no horizontal movement of water could be observed. The state could thus be considered quasi-stable because there existed a pressure gradient for water to leave the cores, but no moisture was able to enter the dry soil. As opposed to runs 2 and 3, when the flow was stopped, and restarted 24 hours later, the water followed the original finger paths and did not enter the regions between the original finger paths. This overall behavior is similar to that reported by *Glass et al.* [1989].

4. Discussion

The simultaneous pressure and saturation measurements clearly show that the nonuniform saturation profile observed after fingering exists for long periods of time. We observe that this nonuniform saturation profile exists for two possible reasons: either because the hysteresis in the pressure-saturation relation allows the pressures but not the saturations to equalize as in runs 2 and 3 or because the flow out of the fingers into the dry soil is extremely slow at these matric potentials, as in run 1. In the rest of this section we focus on the two interesting sidelights of this study: first, the strange behavior where in run

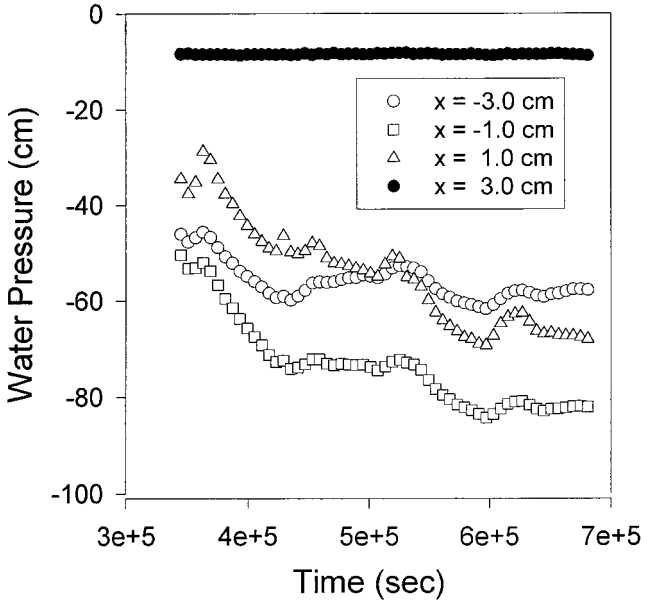

Figure 9. Water pressures versus time for four of the tensiometers during run 1. The legend depicts the x position of each of the tensiometers shown. Solid symbols are for tensiometers within the finger cores, and open symbols are for tensiometers outside the finger cores. The pressures outside the finger cores do not equalize with time.

1 the outside soil remained dry, while in runs 2 and 3 it slowly became wet, and second, the observation of a region of wetter soil being at a higher matric potential than the drier soil adjacent to it.

Why did the rate of fluid transport out of the fingers vary from run 1 to runs 2 and 3? Run 1 was performed under conditions identical to those of runs 2 and 3, except the lights were left on for the first 24 hours of run 1 and the outside weather was much warmer and more humid than during runs 2 and 3. Since the constant temperature room which held the experiments had no humidity control, this leads us to consider the effect of the room vapor pressure.

Assuming that the flow field is uniform in the z direction, the water flux from the finger cores into the dry sand can be written as the sum of the vapor and liquid transport:

$$q_x = \frac{D_v}{\varepsilon}\frac{\partial \rho_v}{\partial x} + K(\theta_l)\frac{\partial \psi}{\partial x} \tag{2}$$

Here q_x is the horizontal flux of water (g/cm^2 s), D_v is the diffusion constant for vapor in the soil (cm^2/s), ρ_v is the mass density of water in the vapor phase (g/cm^3) and is directly related to the vapor pressure, $K(\theta_l)$ is the unsaturated liquid water conductivity (g/cm^2 s), and ψ is the matric potential (centimeters of water). To calculate the lower limit of the water flux out of the finger core, we take the conservative assumption that $K(\theta_l)$ is extremely small at these fluid contents. Assuming that the vapor condenses to liquid behind the vapor front, we can write the conservation of mass equation as

$$\frac{\partial \rho_v}{\partial t} = D_v\frac{\partial^2 \rho_v}{\partial x^2} - \frac{\partial \theta_l}{\partial t} \tag{3}$$

where θ_l is the liquid water content. Since $\rho_v \ll \theta_l$, (3) becomes

$$D_v\frac{\partial^2 \rho_v}{\partial x^2} = \frac{\partial \theta_l}{\partial t} \tag{4}$$

Integrating (4) with respect to x from the initial finger edge, defined as $x = x_e$, to the liquid front, x_f, results in

$$D_v\left.\frac{\partial \rho_v}{\partial x}\right|_{x=x_e} = \frac{dI_l}{dt} \tag{5}$$

where I_l is the cumulative lateral flux from the core of the finger and is equal to

$$I_l = \int_{x_f}^{x_e} \theta_l\, dx \tag{6}$$

To find a solution to (5), we estimate the vapor gradient by

$$\left.\frac{\partial \rho_v}{\partial x}\right|_{x=x_e} = \frac{\rho_{v_s} - \rho_{v_a}}{x_f - x_e} \tag{7}$$

where ρ_{v_s} and ρ_{v_a} are the saturated and ambient mass density of water in the vapor phase, respectively. Next we approximate the cumulative horizontal flux assuming that the moisture decreases linearly with distance to the finger. On the basis of this the cumulative infiltration can be written as

$$I_l = \tfrac{1}{2}\,\theta_{x=x_e}(x_f - x_e) \tag{8}$$

By substituting (8) and (7) into (5), we obtain by integration

$$I_l = \sqrt{D_v(\rho_{v_s} - \rho_{v_a})\theta_{x=x_e}\,t} \tag{9}$$

As expected, the cumulative lateral infiltration is a function of $t^{1/2}$.

To examine if the observed redistribution of water throughout the sand pack is consistent or not with vapor transport, we will compare the observed transport with that calculated with (9). Here we assume that inside the finger the vapor is saturated, while outside the finger the vapor pressure is equal to the ambient vapor pressure. The moisture content outside the finger is initially zero. Hence in (9) the vapor pressure at the edge of the finger at 21°C is 24.5 mbar, which converts to a vapor density of 2.0×10^{-5} g/cm^3. The diffusion constant of vapor in soil is $D_v = 5.6 \times 10^{-2}$ cm^2/s, obtained from the diffusion of water in air ($D_0 = 0.24$ cm^2/s) [*CRC Press*, 1982] and the use of Penman's formula ($D_v = 0.66\, f_A D_0$) [*Hillel*, 1980; *Penman*, 1940], where $f_A = 0.37$ is the air filled porosity. To find the moisture content $\theta_{x=x_e}$, we take the moisture content near the edge of the finger that does not change during the experiment. For run 1 this is 0.03 and for run 2 it is 0.06 g/cm^3. The ambient vapor pressure during run 1 was 18 mbar and 4 mbar during run 2.

The observed flow was obtained with (6) from the measured cross-sectional moisture content data as shown in Figures 3 and 8. For run 1 the cumulative flow was calculated between $x = -5$ and 1 cm and between $x = 3.5$ and 5 cm (Figure 8). For run 2 the area located between $x = -9$ and -5 cm and between $x = -3$ and 6 cm was used (Figure 3).

The observed (symbols) and predicted (lines) cumulative lateral flows are compared for runs 1 and 2 in Figure 10. The predicted cumulative vapor flux for run 1 is in excellent agreement with the calculated values (Figure 10), indicating that sideways moisture movement was caused by the vapor movement. For run 2 the observed sideways flux is slightly higher

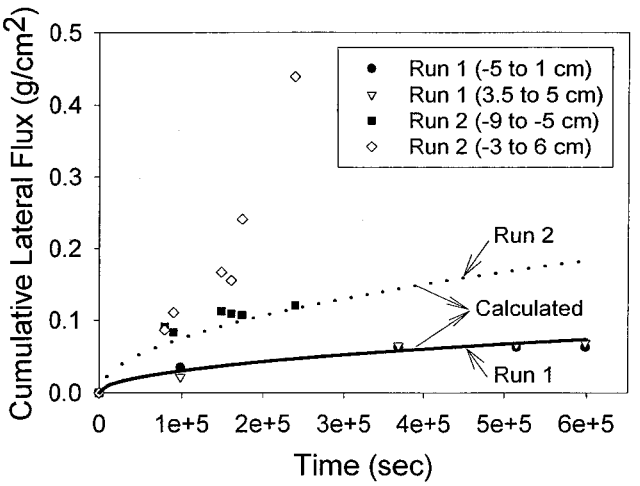

Figure 10. Calculated and observed cumulative lateral flux versus time. The solid line shows the calculated flux for run 1. The dotted line represents the calculated flux for run 2. The legend depicts the observed values for runs 1 and 2. The areas of interest correspond to the x position used for the comparison between the observed and calculated values (Figures 8 and 3, respectively).

than the calculated values in the area located between -9 and -5 cm. However, the calculated flux in the area located between $x = -3$ to 6 cm only compares reasonably well up to 1.0×10^5 s. After that time the cumulative lateral flux is higher than the predicted values and the $t^{1/2}$ relationship in (9) does not hold anymore. Thus, when the two fronts are further apart and then come together, water may be transported as a combination of vapor and liquid water transport.

Another interesting difference between the runs occurred after the infiltration was stopped for a day and then restarted. For run 1, where the pressures did not equalize and portions of the soil remained dry, upon reinfiltration the water followed the old finger cores with roughly the same finger widths. For runs 2 and 3, where the pressures did equalize and no portions of the soil were dry, upon reinfiltration the water followed the cores, but with finger widths greater than the finger spacing (8–10 cm), thus filling the entire chamber. This implies that the recurrence of finger patterns can vary when vapor transport, or any other mechanism, allows the pressures to equalize. A dependence on antecedent conditions has also been observed in the field. In a field study of finger properties over a 1-year period, *Ritsema and Dekker* [1994] found that the widths of the fingers varied between 10 and 50 cm, depending on the sequence of weather conditions.

Raats and van Duijn [1995] have hypothesized that hysteresis in the soil characteristic curve can create a situation where a wetter portion of the soil is at a lower potential than the drier portion of the soil which it contacts. This potential difference will create a driving force for the "nonconventional" flow of water from the drier portion of the soil into the wetter portion. This unique situation is observed upon the ceasing of the infiltration for runs 2 and 3 as the water in the drier soil (outside the cores) is at a higher matric potential than the water in the wetter soil (inside the cores). From Figure 6 we estimate that this potential difference can reach 3 cm for portions of the soil 2 cm apart. The potential gradient for the nonconventional horizontal flow of water from the dry soil into the wet soil can reach a magnitude of roughly $d\psi/dx = 1.5$. Although we have not observed this flow to definitively occur, the horizontal pressure gradient is greater than the vertical potential gradient of $d\psi/dz = 1.0$, owing to gravity. In any case, the water outside the cores tends to be attracted into the cores, mainly as a conduit to drying to the bottom of the chamber. The effects of the finger "pipe" to the groundwater is also evident on drainage, as the higher conductivity enhances drainage. This is in contrast to preferential flow paths caused by macropores where the macropores drain first and then are ineffective in draining the remaining soil.

5. Summary

The simultaneous measurements of pressure and saturation definitively show that the nonuniform moisture profile and flow paths created by fingered flow remain even after the horizontal potentials equalize. This confirms the hypothesis of *Glass et al*. [1989] that hysteresis in the soil characteristic curve promotes the stability of the nonuniform moisture content distribution. Because the pattern is stable, once the preferential paths have been established they tend to control the subsequent flow.

Hysteresis also creates a situation in this system where the wetter portions of the soil can be at a lower potential than the drier portions, resulting in a horizontal driving force for a flow of water from the drier to the wetter soil. It still remains to be seen whether this creates an observable nonconventional flow from the drier to wetter soil. Future work also contains the possibility of whether this situation can also be observed following preferential flow in field soils.

Acknowledgments. We would like to thank Jim Throop and Alon Rimmer for their expertise on video imaging and tensiometer measurements, respectively. We would also like to thank the reviewers for greatly strengthening the arguments in this paper. This work was supported (in part) by the Air Force Office of Scientific Research, USAF, under grant/contract F49620-94-1-0291.

References

Baker, R. S., and D. Hillel, Laboratory tests of a theory of fingering during infiltration into layered soil, *Soil Sci. Soc. Am. J.*, *54*, 20–30, 1990.

Bell, J. L., J. S. Selker, T. S. Steenhuis, and R. J. Glass, Rapid moisture measurements of thin sand slabs, paper presented at International Winter Meeting, Am. Soc. of Agric. Eng., Chicago, Ill., Dec. 18–21, 1990.

Beven, K., and P. Germann, Macropores and water flow in soils, *Water Resour. Res.*, *18*, 1311–1325, 1982.

Brooks, R. H., and A. T. Corey, Hydraulic properties of porous media, *Hydrol. Pap. 3*, 27 pp., Colo. State Univ., Fort Collins, 1964.

CRC Press Inc., *CRC Handbook of Chemistry and Physics*, 62nd ed., Boca Raton, Fla., 1982.

Diment, G. A., and K. K. Watson, Stability analysis of water movement in unsaturated porous materials, 3, Experimental studies, *Water Resour. Res.*, *21*, 979–984, 1985.

Glass, R. J., J.-Y. Parlange, and T. S. Steenhuis, Water infiltration in layered soils where a fine textured layer overlays a coarse sand, in *Infiltration Development and Application*, edited by Y.-U. Fok, pp. 66–81, Am. Soc. of Civ. Eng., Reston, Va., 1987.

Glass, R. J., T. S. Steenhuis, and J.-Y. Parlange, Mechanism for finger persistence in homogeneous, unsaturated, porous media: Theory and verification, *Soil Sci.*, *148*, 60–70, 1989.

Hill, D. E., and J.-Y. Parlange, Wetting front instability in layered soils, *Soil Sci. Soc. Am. Proc.*, *36*, 697–702, 1972.

Hillel, D., *Introduction to Soil Physics*, Academic, San Diego, Calif., 1980.

Liu, Y., T. S. Steenhuis, and J.-Y. Parlange, Formation and persistence of fingered flow fields in coarse grained soils under different moisture contents, *J. Hydrol*., *159*, 187–195, 1994.

Lu, T. X., J. W. Biggar, and D. R. Nielsen, Water movement in glass bead porous media, 2, Experiments of infiltration and finger flow, *Water Resour. Res*., *30*, 3283–3290, 1994.

Parlange, J.-Y., and D. E. Hill, Theoretical analysis of wetting front instability in soils, *Soil Sci*., *122*, 236–239, 1976.

Penman, H. L., Gas and vapor movements in the soil, I, The diffusion of vapors through porous solids, *J. Agric. Sci*., *30*, 437–461, 1940.

Philip. J. R., Horizontal redistribution with capillary hysteresis, *Water Resour. Res*., *27*, 1459–1469, 1991.

Raats, P. A. C., Unstable wetting fronts in uniform and nonuniform soils, *Soil Sci. Soc. Am. Proc*., *37*, 681–685, 1973.

Raats, P. A. C., and C. J. van Duijn, A note on horizontal redistribution with capillary hysteresis, *Water Resour. Res*., *31*, 231–232, 1995.

Ritsema, C. J., and L. W. Dekker, How water moves in a water repellent sandy soil, 2, Dynamics of fingered flow, *Water Resour. Res*., *30*, 2519–2531, 1994.

Selker, J. S., T. S. Steenhuis, and J.-Y. Parlange, Wetting front instability in homogeneous sandy soils under continuous infiltration, *Soil Sci. Soc. Am. J*., *56*, 1346–1350, 1992a.

Selker, J. S., J.-Y. Parlange, and T. S. Steenhuis, Fingered flow in two dimensions, 2, Predicting finger moisture profile, *Water Resour. Res*., *28*, 2523–2528, 1992b.

T. W. J. Bauters, C. J. G. Darnault, J.-Y. Parlange, and T. S. Steenhuis, Department of Agricultural and Biological Engineering, Cornell University, Riley-Robb Hall, Ithaca, NY 14853. (tss1@cornell.edu)

D. A. DiCarlo, Department of Petroleum Engineering Stanford University, Stanford, CA 94305.

(Received July 20, 1998; revised October 15, 1998;
accepted October 16, 1998.)